THE MINIMAL COMPUTATIONAL DOMAIN FOR CAPTURING TAYLOR–GÖRTLER VORTICES IN STREAMWISE-ROTATING CHANNEL FLOW

Zixuan Yang

Department of Mechanical Engineering
University of Minnesota
Minneapolis, MN, 55455, USA
yang4997@umn.edu

Bing-Chen Wang

Department of Mechanical Engineering
University of Manitoba
Winnipeg, MB, R3T 5V6, Canada
Bingchen.Wang@umanitoba.ca

ABSTRACT

In this paper, the minimum computational domain size for correctly capturing Taylor-Görtler (TG) vortices in a streamwise-rotating plane channel is investigated using direct numerical simulations (DNS). To assess the effect of system rotation on the scales of TG vortices, a wide-range of rotation numbers have been tested, varying from $Ro_\tau = 7.5$ to 150. The highest rotation number tested in the current research far exceeds that reported in literature ($Ro_\tau = 30$) by Yang *et al.* (2010). In order to precisely capture TG vorticies, DNS has been performed in a very large box domain of $512\pi h \times 2h \times 8\pi h$, where h is one-half the channel height. A two-layer pattern of TG vortices is observed, and the scales of TG vortices are quantified using the pre-multiplied two-dimensional energy spectra.

INTRODUCTION

Investigations of rapidly rotating turbulent channel flows are fundamentally important for understanding the momentum and energy transfer in rotating machinery. It has been well observed that in a spanwise-rotating channel, large-scale longitudinal Taylor-Görtler vortices appear in pairs in cross-stream planes, which in turn drastically alter flow structures and turbulent statistics (Johnston *et al.*, 1972; Kristoffersen & Andersson, 1993; Grundestam *et al.*, 2008).

In comparison with the spanwise-rotating flows, the large-scale structures in a streamwise-rotating channel are less understood. Wu & Kasagi (2004) performed DNS of a streamwise-rotating turbulent channel flow at low rotation numbers up to $Ro_\tau = \Omega h/u_\tau = 15$ with the streamwise computational domain size varying from $L_1 = 5\pi h$ to $8\pi h$. They observed two-dimensional (2D) large-scale roll cells in the cross-stream direction. Here, Ω represents the angular velocity of the system rotation, u_τ denotes the wall-friction velocity, and h is half the channel height. Weller & Oberlack (2006*a*) set the streamwise computational domain size to $L_1 = 16\pi h$ for $Ro_\tau = 15$ and 20. They observed that the extent of the instantaneous large-scale structures can be as long as the computational domain size in the streamwise direction.

To date, the precise scales of TG vortices are still not clear in a streamwise-rotating channel. The rotation numbers reported in literature have been low or moderate and DNS has been performed based on either small or moderate computational domains. In order to conduct a comprehensive examination of the dynamics and growth of TG vortices in response to the system rotation imposed, a wide range of rotation numbers from $Ro_\tau = 0$ to 150 are tested. The highest rotation number ($Ro_\tau = 150$) tested in this research far exceeds that reported in literature ($Ro_\tau = 30$, Yang *et al.*, 2010). The streamwise domain size is stretched to $L_1 = 512\pi h$ to capture energetic eddies for $Ro_\tau = 150$. This streamwise domain size is significantly larger than that reported in the literature ($16\pi h$, Weller & Oberlack, 2006*b*) for lower rotation numbers.

NUMERICAL ALGORITHM

Let x_1, x_2 and x_3 denote the streamwise, wall-normal and spanwise coordinates, respectively, and u_1, u_2 and u_3 represent velocity components in the corresponding directions. The continuity and momentum equations for an incompressible flow subjected to a streamwise system rotation take the following form

$$\frac{\partial u_i}{\partial x_i} = 0, \tag{1}$$

$$\frac{\partial u_i}{\partial t} + u_k \frac{\partial u_i}{\partial x_k} = -\frac{1}{\rho}\frac{\partial p}{\partial x_i} + \nu \frac{\partial^2 u_i}{\partial x_k \partial x_k} + 2\varepsilon_{1ik}\Omega u_k - \frac{1}{\rho}\frac{\mathrm{d}\Pi}{\mathrm{d}x_1}\delta_{i1}. \tag{2}$$

Here, $p = p_s - \Omega^2(x_2^2 + x_3^2)/2$ represents an effective pressure, which has absorbed the centrifugal force into the static pressure p_s, ε_{ijk} is the Levi-Civita symbol, $\mathrm{d}\Pi/\mathrm{d}x_1$ is a constant streamwise pressure gradient that drives the flow, and δ_{ij} denotes the Kronecker Delta. Periodic boundary conditions are applied to the streamwise and spanwise directions, and no-slip boundary conditions are prescribed at the two solid walls.

Equations (1) and (2) are solved using an in-house pseudo-spectral method code. The grid is evenly spaced in both streamwise and spanwise directions. In the wall-normal direction, the grid is refined in the near-wall region by use of the Chebyshev-Gauss-Lobatto points, i.e. $x_{2,j} = -h\cos(j\pi/N_2)$ for $j = 0, 1, .., N_2$. The velocity and pressure are expanded into Fourier series in the streamwise and spanwise directions, and into Chebyshev polynomial series in the wall-normal direction. The advection terms in momentum equations are calculated in the physical space. Aliasing errors are removed using the $3/2$ rule. A third-order time-splitting method is used for time integration. All numerical simulations were conducted using the Western Canada Research Grid (WestGrid) supercomputing and storage facilities.

TEST CASES

Table 1 summarizes the testing parameters (domain size, grid resolution and rotation number) for 14 test cases. To focus our study on the effects of rotation on turbulence statistics, the length scales of T-G vortices and the proper domain size for capturing energetic eddy motions, the Reynolds number is fixed to $Re_\tau = u_\tau h/\nu = 180$, and a wide range of rotation numbers (for $Ro_\tau = 0$, 7.5, 15, 30, 75, and 150) are considered. Here, ν is the kinematic viscosity. The test cases corresponding to these six rotation numbers are categorized and labeled using six initial letters "O" to "E". The purpose of including case O is for validating our non-rotating channel flow results against those of Hoyas & Jiménez (2006), and this reference test case is designated as "HJ06" hereafter. In the next section, it will be demonstrated that as Ro_τ increases, the streamwise extent of TG vortices increases monotonically, and as a result, it becomes increasingly expensive to perform DNS by using a longer computational domain. In order to examine the influence of the computational domain size on the predicted scales of TG vortices and on the accuracy of turbulence statistical moments obtained in both physical and spectral

Test case	Ro_τ	$L_1 \times L_2 \times L_3$	$N_1 \times N_2 \times N_3$
O	0	$12\pi h \times 2h \times 4\pi h$	$384 \times 128 \times 256$
A	7.5	$32\pi h \times 2h \times 8\pi h$	$1024 \times 128 \times 512$
B	15	$64\pi h \times 2h \times 8\pi h$	$2048 \times 128 \times 512$
C	30	$128\pi h \times 2h \times 8\pi h$	$4096 \times 128 \times 512$
D	75	$256\pi h \times 2h \times 8\pi h$	$8192 \times 128 \times 512$
E0a	150	$5\pi h \times 2h \times 2\pi h$	$160 \times 128 \times 128$
E0b	150	$16\pi h \times 2h \times 4\pi h$	$512 \times 128 \times 256$
E1	150	$32\pi h \times 2h \times 8\pi h$	$1024 \times 128 \times 512$
E2	150	$64\pi h \times 2h \times 8\pi h$	$2048 \times 128 \times 512$
E3	150	$128\pi h \times 2h \times 8\pi h$	$4096 \times 128 \times 512$
E4	150	$256\pi h \times 2h \times 8\pi h$	$8192 \times 128 \times 512$
E5	150	$512\pi h \times 2h \times 8\pi h$	$16384 \times 128 \times 512$
E5a	150	$512\pi h \times 2h \times 2\pi h$	$16384 \times 128 \times 128$
E5b	150	$512\pi h \times 2h \times 4\pi h$	$16384 \times 128 \times 256$

Table 1. Summary of test cases.

spaces, in total, nine different domain sizes (corresponding to "E"-series test cases, E0a–E5b) are compared at $Ro_\tau = 150$. The domain sizes for cases E0a and E0b are kept identical to those used by Wu & Kasagi (2004) and Weller & Oberlack (2006*a*), respectively. In our study of computational domain sizes, seven "E"-series test cases are compared, which can be further divided into two sub-groups. The first sub-group consists of cases E1–E5, which are used for examining the effects of streamwise domain size on the predicted streamwise scales of TG vortices. In these five test cases, the streamwise domain size L_1 increases from $32\pi h$ to $512\pi h$, while the spanwise domain size L_3 is fixed to $8\pi h$. The second sub-group consists of cases E5a, E5b and E5, which are compared for examining the effects of the spanwise computational domain size L_3 on the predicted spanwise scales of TG vortices. In these three test cases, L_3 increases from $2\pi h$ to $8\pi h$, while L_1 is fixed to $512\pi h$. In table 1, N_1, N_2, and N_3 represent the number of grid points in the spectral space in the x_1-, x_2-, and x_3-directions, respectively. The streamwise and spanwise grid resolution for all test cases is fixed to $\Delta_1^+ = 17.7$ and $\Delta_3^+ = 8.9$, respectively. The vertical grid resolution varies from $\Delta_2^+ = 0.054$ at the wall to $\Delta_2^+ = 4.4$ in the channel center. Here, superscript "+" denotes a non-dimensional quantity expressed in wall coordinates based on ν and u_τ. The grid resolution in the present study is similar to that used by Kim *et al.* (1987) for DNS of non-rotating turbulent channel flow at a similar Reynolds number. We further remark that the resolution in the streamwise and spanwise directions does not meet the more stringent criteria ($\Delta_1^+ = 12$ and $\Delta_3^+ = 6$) recommended by Hoyas & Jiménez (2006). However, as demonstrated later in the next section, the statistical results for case O agree well with those in HJ06. Furthermore, because the scales of TG vortices are significantly larger than the grid size, the present resolution is sufficient for studying the scales of TG vortices in a streamwise-rotating turbulent plane-channel flow.

RESULTS

Figure 1 shows the influences of the computational domain size on the predicted profiles of the mean streamwise velocity $\langle u_1 \rangle^+$ and mean spanwise velocity $\langle u_3 \rangle^+$. It is evident from the figure that the results of case O agree well with those of HJ06, confirming that the present numerical algorithm is accurate for performing DNS of turbulent plane-channel flows. As is clear in figure 1(a), similar

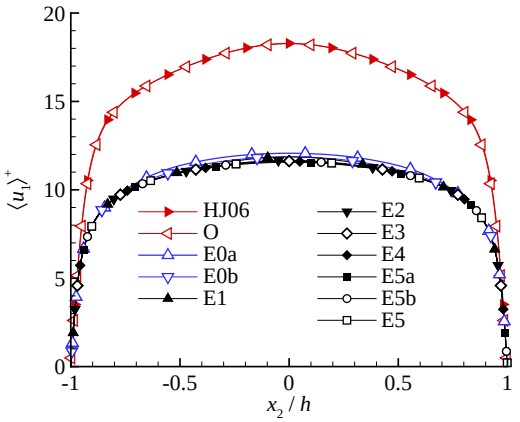

(a) Mean streamwise velocity $\langle u_1 \rangle^+$

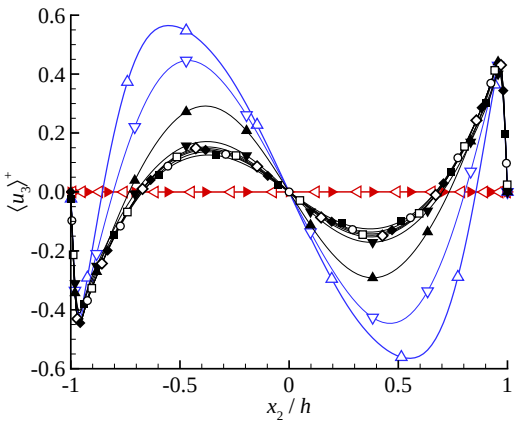

(b) Mean spanwise velocity $\langle u_3 \rangle^+$

Figure 1. Profiles of mean streamwise velocity $\langle u_1 \rangle^+$ and mean spanwise velocity $\langle u_3 \rangle^+$ based on various computational domain sizes.

to that in the non-rotating turbulent plane-channel flow, the profile of $\langle u_1\rangle^+$ in the streamwise-rotating channel is symmetrical about $x_2 = 0$. However, in contrast to the non-rotating plane channel for which $\langle u_3\rangle^+ \equiv 0$, the mean spanwise profile of $\langle u_3\rangle^+$ in the streamwise-rotating channel exhibits a complex pattern of the so-called "(double) S-shaped triple-zero-crossing pattern" (Weller & Oberlack, 2006*a*,*b*).

From figure 1(a), it is clear that although the value of the mean streamwise velocity $\langle u_1\rangle^+$ is slightly over-predicted in case E0a (which has the smallest L_1 value), in general, the predictive accuracy of DNS results based on all different domain sizes is satisfactory. However, as is evident from figure 1(b), in terms of the prediction of the mean spanwise velocity $\langle u_3\rangle^+$, DNS results based on shorter streamwise domain sizes (i.e., cases E0a, E0b, and E1) are inaccurate. In comparison, the results of $\langle u_3\rangle^+$ for cases with longer streamwise domain sizes (i.e., cases E2–E5, E5a, and E5b) all collapse to a single profile.

Figure 2 compares the profiles of Reynolds stresses obtained based on nine different computational domains. For the purpose of comparison, we also show the results of cases O and HJ06 in the figure. From figure 2, the rotating effects can be observed as all six components of the Reynolds stress tensor are non-trivial in the streamwise-rotating channel, while only four are non-trivial in the non-rotating channel. A general observation from figure 2 is that among the six Reynolds stress components, only $\langle u_1'u_2'\rangle^+$ is insensitive to the streamwise computational domain size L_1. In fact, if solely based on $\langle u_1\rangle^+$ and $\langle u_1'u_2'\rangle^+$, it is very tempting to draw a conclusion that $L_1 = 16\pi h$ is sufficient to be the minimal streamwise domain size. However, as is evident from figures 2(a)–(f), in order to correctly predict all six Reynolds stress components, the minimal L_1 value needs to be $64\pi h$, a conclusion that is consistent with the previous analysis of the mean velocity profiles. For instance, in case E0, an additional peak occurs in the profiles of $\langle u_2'u_2'\rangle^+$ and $\langle u_2'u_3'\rangle^+$ at the center of the channel, which is an artifact due to the use of an insufficient streamwise domain size of $L_1 = 5\pi h$. Profiles obtained from cases E5a, E5b, and E5 all collapse, indicating that $L_3 = 2\pi h$ is sufficient for achieving a domain-size-independent solution for Reynolds stresses.

Figure 3(a) demonstrates the 3D isosurfaces of $\overline{\omega_1'}^+$ for case E5, of which only 1/8 streamwise domain size is shown to ensure that vortices can be visualized clearly. Here, $\omega_1' = (\partial u_2'/\partial x_3 - \partial u_3'/\partial x_2)/2$ represents the fluctuating streamwise vorticity and an overbar denotes time-averaging. From Fig. 3(a), it is evident that the TG vortices demonstrated using the isosurfaces of $\overline{\omega_1'}^+$ are elongated in the streamwise direction. In the spanwise direction, positive and negative vorticities alternate, indicating the presence of counter-rotating TG vortex pairs. Figures 3(b) and (c) show the TG vortices in two arbitrary cross-stream (x_2–x_3) planes partially extracted from the 3D domain at $x_1 = 32\pi h$. As is evident from Fig. 3(b), two layers of counter-rotating TG vortex pairs are present in the cross-stream plane. As shown in figure 3(c), at a different spanwise location, only one counterclockwise-rotating vortex with a larger scale is observed, while the scale of clockwise-rotating vortices is much smaller. The two-layer pattern of TG vortices observed in the present streamwise-rotating channel is interesting, which is drastically different from the well-known single-layer TG vortex pattern in a spanwise-rotating channel (Johnston *et al.*, 1972; Kristoffersen & Andersson, 1993). However, there is a common feature: the TG vortices in both streamwise- and spanwise-rotating channels are persistent, streamwise-elongated and appearing in counter-rotating pairs. The observation of the two-layer TG vortex pattern in the current turbulent streamwise-rotating channel flow is similar to the result of Masuda *et al.* (2008), who performed the instability analysis of the laminar flow in a streamwise-rotating channel at a lower Reynolds number.

In order to precisely determine the scales of TG vortices, we consider the pre-multiplied energy spectra ϕ_{ii} for $i = 1$, 2, and 3. Figures 4 and 5 compare the isopleths of ϕ_{ii} for cases E2 and E5 in the x_1–x_3 plane at $x_2 = 0.5h$, respectively. The isopleths are plotted with respect to the streamwise length scale $\lambda_1 = 2\pi/k_1$ and spanwise length scale $\lambda_3 = 2\pi/k_3$. The location of the peak value of the spectral energy density, i.e. $\max(\phi_{ii})$, is marked by a cross symbol. Following Hoyas & Jiménez (2006) and Avsarkisov *et al.* (2014), we show two isopleths for each spectrum. The inner and outer isopleths are quantified by $\phi_{ii} = 0.625\max(\phi_{ii})$ and $\phi_{ii} = 0.125\max(\phi_{ii})$, respectively. The area inside the inner isopleth corresponds to the high-intensity core of energetic eddies. If the chosen computational domain size is too small to capture the complete high-intensity core of eddies, the numerical simulation is considered rather inaccurate for correctly capturing large-scale flow structures. The outer isopleth identifies the scale range of eddies, of which the pre-multiplied 2D energy spectrum decays to 12.5% of its peak value. Although eddies with scales between the inner and outer isopleths are less dominant compared to those within the inner isopleth, they are still considerably energetic. All scales of eddies within the outer isopleth need to be fully captured by using a properly-sized computational domain in order to correctly simulate the flow physics using DNS.

As is evident from figure 4, with respect to all three pre-multiplied 2D energy spectra (i.e., ϕ_{11}, ϕ_{22} and ϕ_{33}), both the inner and outer isopleths are open in case E2, indicating that neither the outer border nor the high-intensity core of energetic eddies is properly contained by the computational domain. The energy cascade beyond the computational domain size has been artificially chopped off in a very abrupt manner. It is known from figure 5 that in order to capture the outer border of energetic eddies at $Re_\tau = 150$, the minimum streamwise and spanwise domain sizes need to be kept at $L_1 = 512\pi h$ and $L_3 = 8\pi h$, respectively. Therefore, only the computational domain of case E5 is capable of correctly capturing all energetic eddies. In contrast, the streamwise computational domain sizes of cases E1–E4 are insufficient for capturing a closed isopleth of $\phi_{11} = 0.125\max(\phi_{11})$, while the spanwise computational domains of cases E5a and E5b are too small to contain the complete isopleth of $\phi_{33} = 0.125\max(\phi_{33})$. It should be indicated that these conclusions are dependent on the arbitrary choice of the threshold value (i.e., $0.125\max(\phi_{ii})$) for quantifying the dominant eddies. If we may increase this threshold value, then a smaller computational domain size could also be judged as satisfactory for capturing all energetic eddies.

To avoid the above ambiguity in the determination of the scales of the high-intensity core and outer border of energetic eddies by using the arbitrary threshold values recommended by Hoyas & Jiménez (2006) and Avsarkisov *et al.* (2014), we may instead directly consider the characteristic streamwise and spanwise length scales of TG vortices corresponding to $\max(\phi_{ii})$, which are denoted as ξ_i and ζ_i, respectively. As can be seen in figure 5, the peaks of ϕ_{11}, ϕ_{22} and ϕ_{33} for case E5 occur at $[\xi_1^+, \zeta_1^+] = [48000, 430]$, $[\xi_2^+, \zeta_2^+] = [12000, 270]$ and $[\xi_3^+, \zeta_3^+] = [3400, 230]$, respectively. As shown previously in DNS studies of non-rotating turbulent channel flow (Hoyas & Jiménez, 2006) and turbulent Couette flow (Avsarkisov *et al.*, 2014), the scales corresponding to the most energetic eddies derived from the three independent ϕ_{ii} values do not have to be identical due to the nonlinear interactions between different scales of 3D turbulent eddy motions.

Figure 6 compares the locations of $[\xi_i^+, \zeta_i^+]$ in the λ_1^+–λ_3^+ plane for cases E1–E5, E5a, and E5b. Because the computational domain is the largest in case E5 among these seven test cases (see table 1), the predicted streamwise and spanwise characteris-

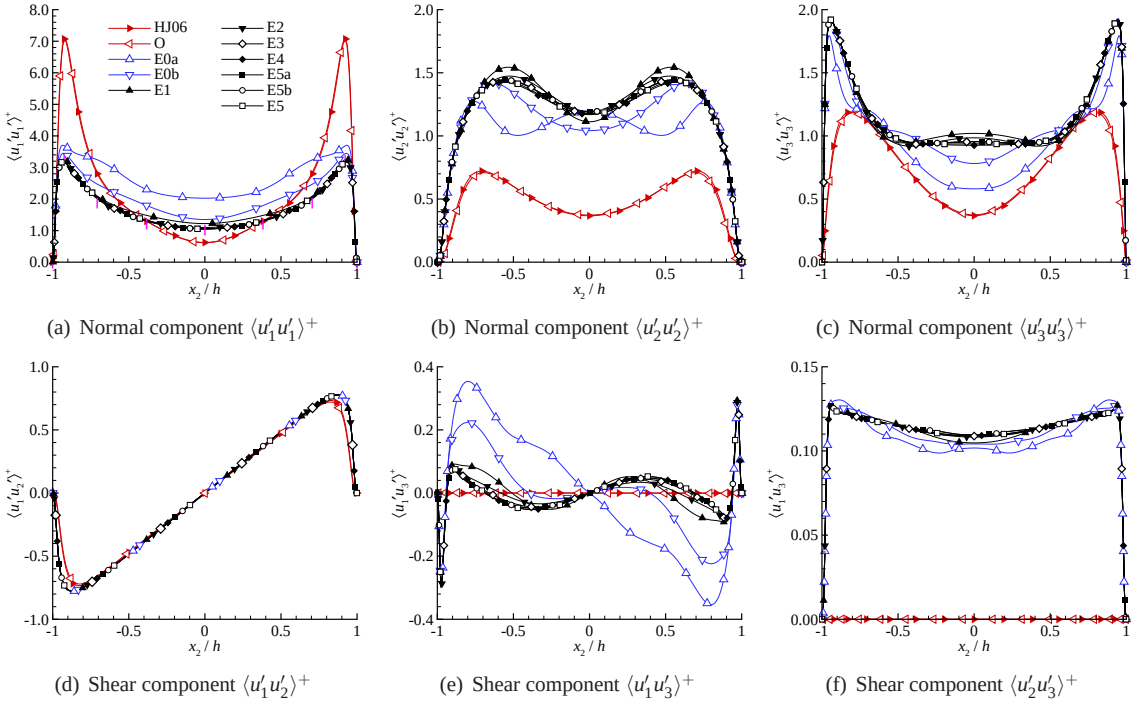

(a) Normal component $\langle u_1'u_1'\rangle^+$ (b) Normal component $\langle u_2'u_2'\rangle^+$ (c) Normal component $\langle u_3'u_3'\rangle^+$

(d) Shear component $\langle u_1'u_2'\rangle^+$ (e) Shear component $\langle u_1'u_3'\rangle^+$ (f) Shear component $\langle u_2'u_3'\rangle^+$

Figure 2. Profiles of Reynolds stresses based on various computational domain sizes.

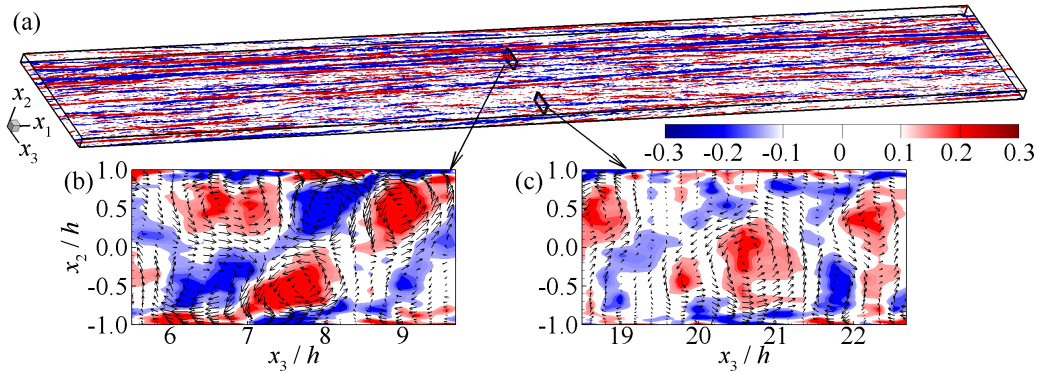

Figure 3. Elongated TG vortex structures for case E5. (a): time-averaged 3D isosurfaces of $\overline{\omega_1'}^+ = \pm 0.02$. Blue and red colors represent negative and positive vorticities, respectively. Only 1/8 of the streamwise domain size of case E5 is shown. (b) and (c): local TG vortex structures visualized in two arbitrary cross-stream (x_2–x_3) planes partially extracted from the 3D domain at streamwise location $x_1 = 32\pi h$. The contours of $\overline{\omega_1'}^+$ are superimposed by the time-averaged velocity vectors composed of $\bar{u}_2$ and $\bar{u}_3$. The vectors are shown at every eight spanwise grid points and every four wall-normal points to ensure a clear view of the velocity field.

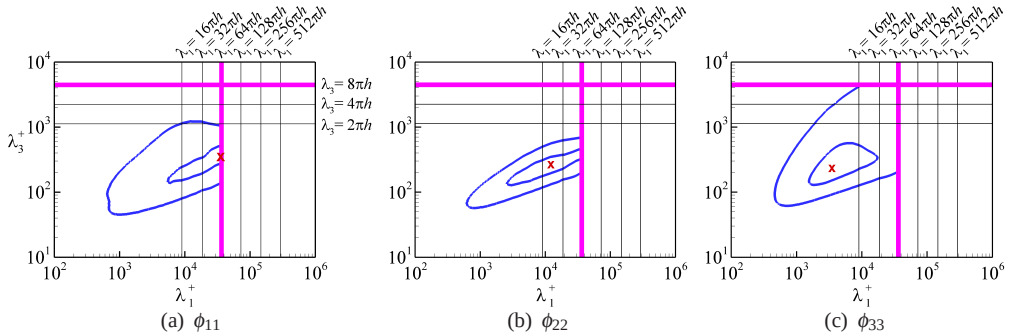

(a) ϕ_{11} (b) ϕ_{22} (c) ϕ_{33}

Figure 4. Isopleths of pre-multiplied 2D energy spectra ϕ_{ii} in plane $x_2/h = 0.5$ for case E2. The cross symbol "×" indicates the location of the maximum pre-multiplied energy spectra. Vertical lines indicate the streamwise computational domain size for cases E1–E5 (corresponding to $\lambda_1 = 32\pi h$–$512\pi h$), and horizontal lines indicate the spanwise computational domain size for cases E5a, E5b and E5 (corresponding to $\lambda_3 = 2\pi\, h$, $4\pi\, h$ and $8\pi\, h$, respectively). The thick lines highlight the computational domain size for case E2.

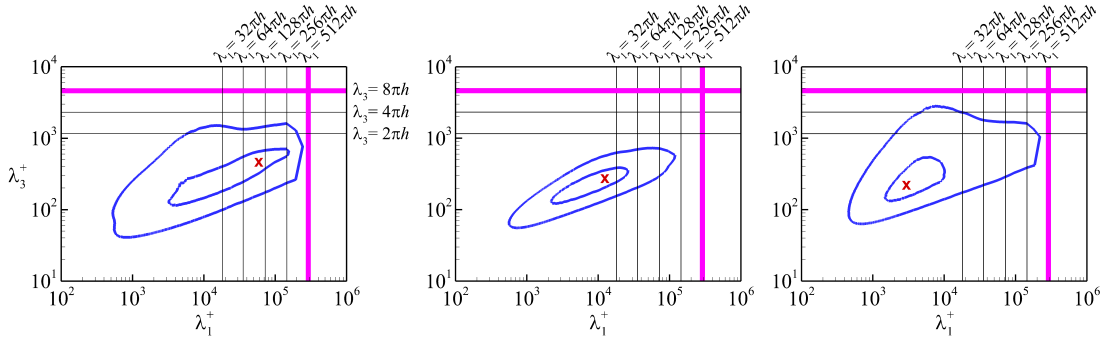

(a) ϕ_{11} (b) ϕ_{22} (c) ϕ_{33}

Figure 5. Isopleths of pre-multiplied 2D energy spectra ϕ_{ii} in plane $x_2/h = 0.5$ for case E5. The thick lines highlight the computational domain size for case E5. See figure 4 for the detailed caption.

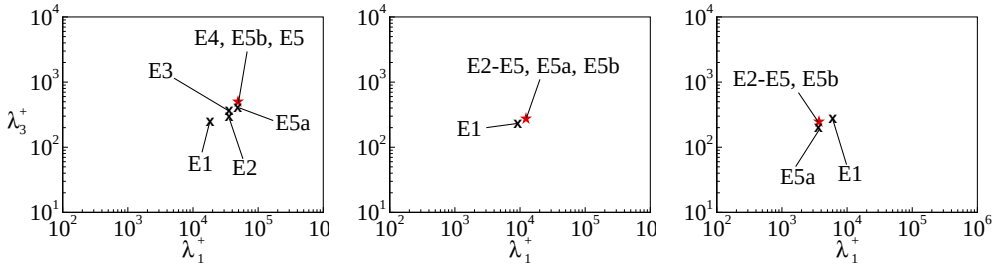

(a) $[\xi_1^+, \zeta_1^+]$ for max(ϕ_{11}) (b) $[\xi_2^+, \zeta_2^+]$ for max(ϕ_{22}) (c) $[\xi_3^+, \zeta_3^+]$ for max(ϕ_{33})

Figure 6. Locations of $[\xi_i^+, \zeta_i^+]$ in the λ_1^+–λ_3^+ plane for cases E1–E5, E5a, and E5b. The values of ξ_i^+ and ζ_i^+ represent the characteristic streamwise and spanwise scales (non-dimensionalized using the wall unit ν/u_τ) of TG vortices corresponding to the peak value of ϕ_{ii}. The red star labels the result for case E5.

tic length scales of TG vortices as represented by the values of ξ_i^+ and ζ_i^+ are not artificially altered by the insufficient computational domain size. In the following context, we will further assess the accuracy of DNS conducted with different domain sizes by comparing the predicted values of ξ_i^+ and ζ_i^+ against those of case E5 (indicated by the red star symbol in figure 6). From figure 6, it is evident that the locations of $[\xi_i^+, \zeta_i^+]$ for cases E4, E5b, and E5 are collocated, indicating that a streamwise–spanwise domain size of $L_1 \times L_3 = 256\pi h \times 4\pi h$ is sufficient for achieving a domain-size-independent result of $[\xi_i^+, \zeta_i^+]$. In other cases, the values of ξ_i^+ and ζ_i^+ are misidentified partially or even completely. It is interesting to observe from figure 6(a) that if the streamwise domain size is not large enough (as in cases E1–E3), neither the streamwise scale ξ_1^+ nor the spanwise scale ζ_1^+ is precisely predicted. In contrast, the spanwise computational domain size influences only the predictive spanwise scale of TG vortices. As shown in figures 6(a)–(c), in comparison with case E5, although the values of ξ_1^+, ξ_2^+, and ξ_3^+ are precisely predicted in case E5a, the values of ζ_1^+ and ζ_3^+ are slightly underpredicted owing to its overly small spanwise domain size.

The effects of the rotation number on the scales of the TG vortices can be studied by comparing cases O, A, B, C, D, and E5, in which the rotation number is 0, 7.5, 15, 30, 75, and 150, respectively (table 1). The values of ξ_i^+ and ζ_i^+ at various rotation numbers are compared in figures 7(a) and 7(b), respectively. The resultant values from DNS for $Ro_\tau = 0.0$, i.e. $\xi_1^+ = 670$ and $\zeta_1^+ = 240$, are consistent with those given in del Álamo & Jiménez (2003). Because TG vortices appear due to imposed system rotation, the values of ξ_i^+ and ζ_i^+ in a streamwise-rotating channel (for $Ro_\tau \geq 7.5$) are significantly larger than those in the non-rotating channel (for $Ro_\tau = 0.0$). From figures 7(b), it is striking that as the rotation number increases

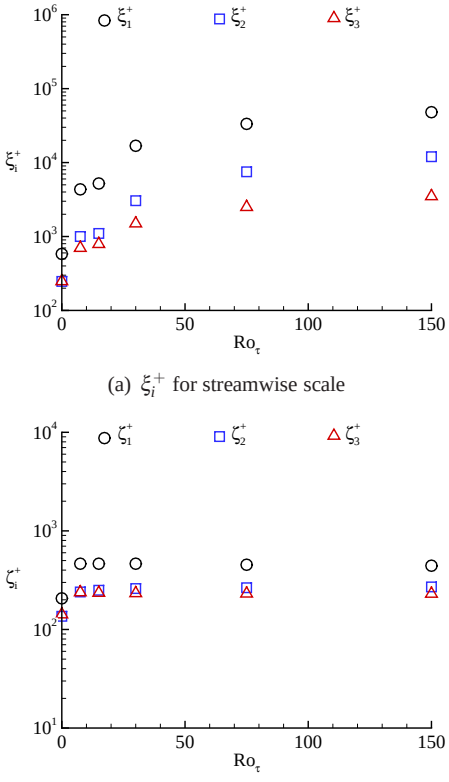

(a) ξ_i^+ for streamwise scale

(b) ζ_i^+ for spanwise scale

Figure 7. The values of ξ_i^+ and ζ_i^+ corresponding to the peak of ϕ_{ii} at various rotation numbers.

drastically from $Ro_\tau = 7.5$ to 150, the values of the characteristic spanwise scales of TG vortices remain almost constant corresponding to $\zeta_1^+ = 430$, $\zeta_2^+ = 270$, and $\zeta_3^+ = 230$. An explanation for this interesting observation is that as shown in figures 3(b) and 3(c), the TG vortices are of a quasi-circular shape in a cross-stream (x_2–x_3) plane, and therefore, the spanwise and vertical scales of the TG vortices are bounded by the channel height. In sharp contrast to the characteristic spanwise scales of TG vortices (figure 7b), the characteristic streamwise scales ξ_i^+ of TG vortices inferred from all pre-multiplied 2D energy spectra from figure 7(a) increase monotonically as Ro_τ increases from 7.5 to 150. This leads to a conclusion that as the rotation number increases, the streamwise computational domain size needs to be extended accordingly in order to correctly perform DNS of a streamwise-rotating turbulent channel flow. In the current literature, DNS of streamwise-rotating turbulent channel flows is limited to low and moderate rotation numbers up to $Ro_\tau = 30$ (Yang *et al.*, 2010), insofar as the rotation effect on the minimal streamwise domain size has not been fully investigated. The importance of the above conclusion on the streamwise computational domain size can be further demonstrated using the example of case E0b, in which the streamwise domain is set to $L_1 = 16\pi h$ following Weller & Oberlack (2006*a*). This streamwise domain size is seemingly long enough, especially when it is compared with that used for DNS of the classical non-rotating turbulent plane channel flow at the same Reynolds number of $Re_\tau = 180$ (e.g., L_1 was set to $4\pi h$ in Moser *et al.* 1999 and $12\pi h$ in Álamo & Jiménez 2003). With this streamwise domain size of case E0b, DNS successfully predicts turbulence statistics and the scales of TG vortices at $Ro_\tau = 20$ (Weller & Oberlack, 2006*a*), but fails if all three criteria would be considered at the highest rotation number tested here for $Ro_\tau = 150$ (even a correct prediction of the basic mean velocity profile is impossible in this case, see figure 1b).

Conclusions

DNS of streamwise-rotating turbulent channel flow has been performed to investigate the effect of system rotation on the large-scale vortices and the concomitant minimal computational domain required for correctly capturing them. Analysis of the results is based on a comparative study of 14 test cases, which are of different domain sizes and cover a wide range of rotation numbers varying from $Ro_\tau = 0$ to 150. It is worth noting that the highest rotation number ($Ro_\tau = 150$) tested in this research far exceeds the highest rotation number ($Ro_\tau = 30$) reported in the literature (Yang *et al.*, 2010), which facilitates a comprehensive examination of the dynamics and growth of TG vortices in response to the increase of the rotation number.

It is interesting to observe that the TG vortices exhibit a two-layer streamwise-elongated counter-rotating pattern. As the rotation number increases, the spanwise scale of the TG vortices remains stable, whereas the streamwise scale increases monotonically. As a result of the extremely high rotation number tested, the streamwise domain size needs to be stretched to $L_1 = 512\pi h$ in order to capture all energetic eddies. This streamwise domain size is significantly larger than that reported in the literature for lower rotation numbers.

It is observed that the minimal computational domain depends strongly on the specific physical quantity under investigation. For instance, for a streamwise-rotating flow at $Ro_\tau = 150$, if the focus is on the predictive accuracy of $\langle u_1 \rangle^+$ and $\langle u_1' u_2' \rangle^+$, a minimal streamwise domain size of $L_1 = 16\pi h$ is sufficient. However, in order to correctly predict the mean spanwise velocity $\langle u_3 \rangle^+$ and all six Reynolds stress components, the minimal L_1 value needs to be increased to $L_1 = 64\pi h$. This difference is caused by the Coriolis forces which induce secondary flows of different modes.

In general, we believe a careful selection of the computational domain size should be solidly based on evidences from both physical and spectral spaces. For this reason, three criteria have been used for judging a domain-size-independent solution: (1) analysis of turbulence statistics in the physical space (to ensure that statistical moments of the velocity field are independent of the computational domain in use); (2) a proposed method which directly assesses the characteristic length scales of TG vortices (to ensure that these vortex scales are independent of the computational domain in the λ_1^+–λ_3^+ plane); and (3) examination of the pre-multiplied 2D energy spectra (to ensure that all energetic eddies are fully captured based on pre-defined spectral energy threshold values. The conclusions from these three criteria are not necessarily consistent, and a conservative method for judging a domain-size-independent solution should be based on satisfying all of these three criteria.

REFERENCES

del Álamo, J. C. & Jiménez, J. 2003 Spectra of the very large anisotropic scales in turbulent channels. *Phys. Fluids* **15** (6), L41–L44.

Avsarkisov, V., Hoyas, S., Oberlack, M. & García-Galache, J. P. 2014 Turbulent plane Couette flow at moderately high Reynolds number. *J. Fluid Mech.* **751**, R1.

Grundestam, O., Wallin, S. & Johansson, A.V. 2008 Direct numerical simulations of rotating turbulent channel flow. *J. Fluid Mech.* **598**, 177–199.

Hoyas, S. & Jiménez, J. 2006 Scaling of the velocity fluctuations in turbulent channels up to Re_τ= 2003. *Phys. Fluids* **18** (1), 011702.

Johnston, J. P., Halleen, R. M. & Lezius, D. K. 1972 Effects of spanwise rotation on the structure of two-dimensional fully developed turbulent channel flow. *J. Fluid Mech.* **56**, 533–559.

Kim, J., Moin, P. & Moser, R. 1987 Turbulence statistics in fully developed channel flow at low Reynolds number. *J. Fluid Mech.* **177**, 133–166.

Kristoffersen, R. & Andersson, H. I. 1993 Direct simulations of low-Reynolds-number turbulent flow in a rotating channel. *J. Fluid Mech.* **256**, 163–197.

Masuda, S., Fukuda, S. & Nagata, M. 2008 Instabilities of plane Poiseuille flow with a streamwise system rotation. *J. Fluid Mech.* **603**, 189–206.

Oberlack, M., Cabot, W., Reif, B. A. P. & Weller, T. 2006 Group analysis, direct numerical simulation and modelling of a turbulent channel flow with streamwise rotation. *J. Fluid Mech.* **562**, 383–403.

Recktenwald, I., Weller, T., Schröder, W. & Oberlack, M. 2007 Comparison of direct numerical simulations and particle-image velocimetry data of turbulent channel flow rotating about the streamwise axis. *Phys. Fluids* **19** (8), 085114.

Weller, T. & Oberlack, M. 2006*a* DNS of a turbulent channel flow with streamwise rotation – investigation on the cross flow phenomena. In *Direct and Large-Eddy Simulation VI* (ed. E. Lamballais, R. Friedrich, B. J. Geurts & O. Métais), pp. 241–248. Springer.

Weller, T. & Oberlack, M. 2006*b* DNS of a turbulent channel flow with streamwise rotation – study of the reverse effect of the cross flow. *Proc. Appl. Math. Mech.* **6**, 553–554.

Wu, H. & Kasagi, N. 2004 Effects of arbitrary directional system rotation on turbulent channel flow. *Phys. Fluids* **16**, 979–990.

Yang, Y.-T., Su, W.-D. & Wu, J.-Z. 2010 Helical-wave decomposition and applications to channel turbulence with streamwise rotation. *J. Fluid Mech.* **662**, 91–122.